

Observational constraints on the linear fluctuation growth rate

Cinzia Di Porto

Dipartimento di Fisica “E. Amaldi”, Università degli Studi “Roma Tre”

Luca Amendola

INAF/Osservatorio Astronomico di Roma, Via Frascati 33

00040 Monte Porzio Catone (Roma), Italy

(Dated: October 25, 2018)

Several experiments in the near future will test dark energy through its effects on the linear growth of matter perturbations. It is therefore important to find simple and at the same time general parametrizations of the linear growth rate. We show that a simple fitting formula that generalizes previous expressions reproduces the growth function in models that allow for a growth faster than standard, as for instance in scalar-tensor models. We use data from galaxy and Lyman- α power spectra to constrain the linear growth rate. We find $\gamma = 0.6^{+0.4}_{-0.3}$ for the growth rate index and $\eta = 0.0^{+0.3}_{-0.2}$ for the additional growth parameter we introduce.

I. INTRODUCTION

After several years from the first works [1, 2], the evidence of dark energy (DE) still rests primarily on background quantities like the luminosity distance and the angular diameter distance [3, 4, 5]. Only recently the cross-correlation of the integrated Sachs-Wolfe effect with the large scale structure yielded an independent proof of the existence of dark energy that rely on the linear growth of the gravitational potential [6]. In the future, galaxy and Lyman- α power spectra at high redshift and weak lensing surveys from ground and from space will offer the opportunity to test competing dark energy models to a very high precision using a mix of background, linear and non-linear indicators [7, 8].

In order to use the growth rate of linear fluctuations as a test of DE, it is however necessary to formulate simple expressions that embody a large class of models, so as to provide observers with a practical tool to analyse the data. This procedure has proved most convenient with the equation of state of DE, whose parametrizations afford the community to quickly compare the different experiments and to optimize the design of further surveys (see eg [9]).

Since many years it has been known that a good approximation to the growth rate of the linear matter density contrast δ in standard models of gravity and dark matter is given by the simple expression [10, 11]

$$s \equiv \frac{\delta'}{\delta} \approx \Omega_m^\gamma, \quad (1)$$

where the prime stands for derivative with respect to $\log a$ and where $\gamma \approx 0.55$. In [12] it was found that this growth rate also accounts for coupled dark energy at small z and small coupling β (see definition below) with $\gamma \approx 0.56(1 - 2.55\beta^2)$. The formula works quite well also in the case in which DE is described by a mildly varying EOS $w(z)$ when generalized with [13] $\gamma \approx 0.55 + 0.05(1 + w(z = 1))$.

However, this formula has an obvious drawback: assuming a constant or weakly varying $\gamma > 0$, it implies $s \leq 1$ at all epochs since in standard cosmology the matter density parameter is always $0 \leq \Omega_m \leq 1$. More exactly, if γ is a constant, then s is always either smaller or larger than unity. Therefore, this fit is unable to test for deviations from the standard paradigm of fluctuation growth, which assumes $s = 1$ for the matter-dominated universe at high redshifts. This assumption is of course dangerous in view of the multitude of dark energy or modified gravity models currently being studied and should not be taken for granted without serious scrutiny.

In this paper we show first that the $s > 1$ behavior takes place in one of the simplest class of modified gravity theories, namely scalar-tensor models or their Einstein frame counterparts, and then we introduce a simple new fitting formula that generalizes eq. (1). We note that a similar faster-than-standard growth has been found also in TeVeS modified gravity models [14]. Finally, we compare our fitting formula with the (scanty) data available at the present.

II. THE GROWTH FUNCTION IN SCALAR-TENSOR THEORIES

In this section we show that generically $s > 1$ at early times and $s < 1$ at late times in a simple class of modified gravity theories.

Let us consider a generic scalar-tensor model in Einstein frame. It is well-known that in the Einstein frame, the frame in which the gravitational equations are in the Einsteinian form while matter is not conserved, the scalar degree

of freedom of a scalar-tensor theory acts as a new force on matter, as expressed by the new conservation equations (here we use subscripts c for CDM, b for baryons, ϕ for the scalar field, and γ for radiation) [15, 16, 17]

$$T_{\nu;\mu(c)}^\mu = -C_c(\phi)T_{(c)}\phi_{;\mu}, \quad (2)$$

$$T_{\nu;\mu(b)}^\mu = -C_b(\phi)T_{(b)}\phi_{;\mu}, \quad (3)$$

$$T_{\nu;\mu(\phi)}^\mu = [C_b(\phi)T_{(b)} + C_c(\phi)T_{(c)}]\phi_{;\mu}, \quad (4)$$

$$T_{\nu;\mu(\gamma)}^\mu = 0, \quad (5)$$

where for generality we assumed that the coupling functions depend on the species (while radiation remains uncoupled because it is conformally invariant). In a FRW metric with scale factor a these equations become (we assume flat space throughout)

$$\begin{aligned} \ddot{\phi} + 3H\dot{\phi} + V_{,\phi} &= \kappa(\beta_c\rho_c + \beta_b\rho_b), \\ \dot{\rho}_c + 3H\rho_c &= -\kappa\beta_c\rho_c\dot{\phi}, \\ \dot{\rho}_b + 3H\rho_b &= -\kappa\beta_b\rho_b\dot{\phi}, \\ \dot{\rho}_\gamma + 4H\rho_\gamma &= 0, \\ 3H^2 &= \kappa^2(\rho_b + \rho_c + \rho_\phi), \end{aligned} \quad (6)$$

where $\kappa^2 = 8\pi G$, $\beta_c = C_c/\kappa$, $\beta_b = C_b/\kappa$, $H = \dot{a}/a$ (note that we use a coupling β which is $\sqrt{2/3}$ the β used in ref. [17]). Then we have immediately

$$\rho_{c,b} = \rho(0)_{c,b}a^{-3} \exp\left\{-\int \beta_{c,b}(\phi)d\phi\right\}. \quad (7)$$

To simplify the analysis and to satisfy local gravity constraints we put from now on $\beta_b = 0$ and $\beta_c = \beta = const.$

As it has been shown in refs. [17], for $\beta < \sqrt{3/2}$ the standard matter era that precedes the final acceleration is replaced in this coupled model by an epoch in which the energy density fractions Ω_m, Ω_ϕ of matter and field are constant and equal to

$$\Omega_\phi = \frac{2}{3}\beta^2, \quad (8)$$

and $\Omega_m = 1 - \Omega_\phi$. During this epoch one has $\phi' = 2\beta$ (the prime stands for $d/d\log a$) and the scale factor grows as $a \sim t^{\frac{2}{3(1+w_e)}}$ with $w_e = 2\beta^2/3$ (these values are approximated since are obtained neglecting both baryons and radiation). This new matter era has been denoted as ϕ MDE in previous works. This occurs when the potential is negligible with respect to the field kinetic energy. Since the potential is dominating the final accelerated epoch, it is clear that the ϕ MDE generically will take place before acceleration and, of course, after the radiation era. This in fact is what has been observed in several numerical and analytical investigations, for instance in the case of exponentials and inverse power-law potentials $V(\phi) = A\phi^{-n}$ [18]. In the Jordan frame, where matter is conserved, the ϕ MDE corresponds to the standard solution of the Brans-Dicke original theory (which is derived in absence of a potential)

$$a_J \sim t^{\frac{2+2\omega}{4+3\omega}}, \quad (9)$$

upon the substitution

$$\beta^2 = \frac{1}{2(3+2\omega)}. \quad (10)$$

Therefore, the ϕ MDE is quite a generic feature of scalar-tensor models and it also shows up in some $f(R)$ models [19]. We now show that during ϕ MDE the growth of fluctuations is faster than in a standard matter era. In ref. [20] it has been shown that the perturbation equations in the sub-horizon regime is

$$\delta_c'' + \left(1 + \frac{\mathcal{H}'}{\mathcal{H}} - \beta_c\phi'\right)\delta_c' - \frac{3}{2}(\gamma_{cc}\delta_c\Omega_c + \gamma_{bc}\delta_b\Omega_b) = 0, \quad (11)$$

where again the prime stands for derivation with respect to $\log a$, and where $\gamma_{ij} = 1 + 2\beta_i\beta_j$ and \mathcal{H} is the conformal Hubble function $\mathcal{H} \equiv aH$. We assume the baryon component to be negligible. Then the fluctuation equation can be solved analytically during the ϕ MDE:

$$\delta \sim a^{1+2\beta^2}, \quad (12)$$

from which it appears that $s = 1 + 2\beta^2$. In the Jordan frame, the growth rate is instead

$$\delta_J \sim a^{\frac{2+\omega}{1+\omega}} \sim a^{\frac{1+2\beta^2}{1-2\beta^2}}, \quad (13)$$

which also gives a rate larger than unity. When the ϕ MDE ends and acceleration takes over, the rate s declines steadily to zero as in standard cases. Therefore, as we anticipated, s goes from a value larger than unity to a value smaller than unity.

III. A GENERALIZED FIT

We now proceed to find a convenient fit to the full evolution of $\delta(a)$ for the coupled models introduced in the previous section. In the standard scenario δ obeys the equation

$$\delta''(\alpha) + \left(1 + \frac{\mathcal{H}'}{\mathcal{H}}\right)\delta'(\alpha) - \frac{3}{2}\Omega_m\delta(\alpha) = 0, \quad (14)$$

where

$$\frac{\mathcal{H}'}{\mathcal{H}} = -\frac{1}{2}(1 + 3w_\phi(\alpha)\Omega_\phi(\alpha)) = -\frac{1}{2}(1 + \frac{\Omega'_m}{\Omega_m}) \quad (15)$$

The solution can then be approximated as

$$\delta(\alpha) = e^{\int_0^\alpha d\alpha' \Omega_m(\alpha')^\gamma}. \quad (16)$$

In our modified gravity eq. (14) becomes

$$\delta'' + \left(1 + \frac{\mathcal{H}'}{\mathcal{H}} - \beta\phi'\right)\delta' - \frac{3}{2}\Omega_m(1 + 2\beta^2)\delta = 0. \quad (17)$$

One simple possibility would be to generalize (16) as

$$\delta(\alpha) = e^{\int_0^\alpha d\alpha' \Omega_m(\alpha)^\gamma(1+c\beta^2)}, \quad (18)$$

with c a parameter to be determined by a least square fit. The choice of a β^2 behavior is suggested by the fact that the ϕ MDE depends only on β^2 . However, this new fit is not very practical because it contains the function $\Omega_m(\alpha)$ that should be obtained by numerically integrating the background equations and therefore depends on the field potential. To overcome this difficulty, we propose to use instead the *standard expression* for Ω_m :

$$\Omega_m^{(s)}(a) = \frac{\Omega_{m,0}}{\Omega_{m,0} + (1 - \Omega_{m,0})a^{-3\hat{w}}}, \quad (19)$$

where $\hat{w} = (\log a)^{-1} \int w(a)da/a$ and the subscript 0 denotes the present time. For the coupled dark energy model we are considering here, we approximate $w(z) \approx w_\phi(z=0)$; although one could easily expand $w(z)$ to higher orders, our approximation is sufficient to show that our generalized fit works well. Therefore we define the rate

$$s \equiv \Omega_m^{(s)}(\alpha)^\gamma(1 + c\beta^2). \quad (20)$$

In this way, the growth rate can be parametrized by $\Omega_{m,0}$, γ , and the combination $\eta \equiv c\beta$, plus the parameters that enter $w(z)$. Now, even in the limit $\Omega_m \rightarrow 1$ one has $s \neq 1$. In the next section we show that this generalized fit is indeed a good approximation. Since we know that during the ϕ MDE (i.e. at high z , for which $\Omega_m^{(s)} \approx 1$) one has $s = 1 + 2\beta^2$ we can anticipate that the result will be close to $c \approx 2$.

Concluding this section we note that eq. (20) should be seen for what it is, i.e. a phenomenological fit. The relation of $\Omega_{m,0}$, $w(z)$, γ and η to the underlying theory will of course depend on the theory itself. For instance, the identification of $\Omega_{m,0}$ with the presently clustered mass in galaxies and clusters of galaxies is actually a model-dependent assumption; if gravity is not standard this assumption is likely to be incorrect. All we are assuming here is that the Friedmann equation can be written as the sum of two components, one that dilutes as $\Omega_{m,0}a^{-3}$ and the other as $(1 - \Omega_{m,0})a^{-3(1+\hat{w})}$; if the gravitational equations are not standard, one has to define $\Omega_m(a)$ such that the above parametrization is still valid. The advantage of using (19-20) is that both background and linear growth are fitted by the same expression for $w(a)$; that is, once one adopts a prescription for $w(a)$ one can fit all the data by simply adding the two parameters γ and η (plus possibly further parameters to account for the anisotropic stress, see eg. [21]). Of course, in principle one could proceed in different ways: for instance, one could parametrize $\Omega_m(a)$ so that values larger than unity in the past were allowed so as to force $s > 1$. Trivially, in fact, our parametrization above could be written equivalently defining a new density $\Omega_m \equiv \Omega_m^{(s)}(1 + \eta)^{1/\gamma}$; this density parameter would however not be the same that appears in the Friedmann equation.

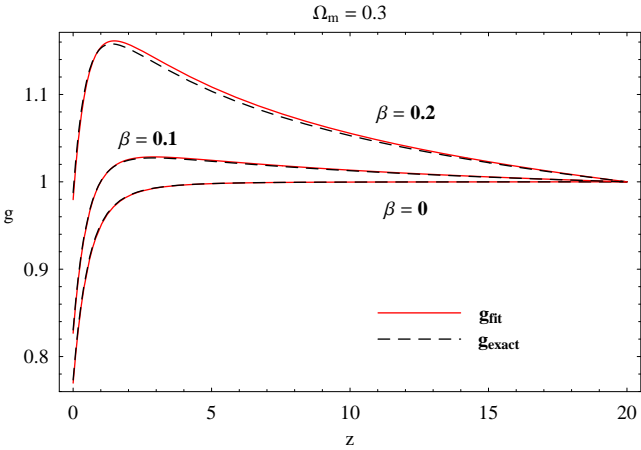


Figure 1: We compare the functions $g_{fit} \equiv \delta_{fit}/a$ (red solid curves), given by the fitting formula (18) with the best fit (parameters $\gamma=0.56$, $c=2.1$) for two different values for β , to the exact solutions $g_{exact} \equiv \delta_{exact}/a$ (black dashed curves) of the differential equation (14) for the growth rate. The curve for $\beta=0$ also gives the standard best fit (i.e. for $c=0$). All curves are normalized at unity at $z=20$. The cases $\beta=0, 0.2$ are for an exponential potential, the case $\beta=0.1$ for $V \sim 1/\phi$.

IV. COMPARING THE FIT TO THE NUMERICAL RESULTS.

We solved numerically the background equations of the system (6) choosing an exponential form for the potential $V(\phi)$ and neglecting the fraction of baryons and radiation. Then we solved numerically the differential equation (17), thus obtaining a solution (that we denote δ_{exact}) which depends on the value of the coupling constant β . For β ranging between 0 and $1/2$, we found that the values of the parameters γ , c appearing in (20), which produce the best fit to δ_{exact} are $\gamma=0.56$ and $c=2.1$. Our best fit is therefore

$$\delta_{fit}(\alpha, \beta) \equiv e^{\int_0^\alpha d\alpha' \Omega_m^{(s)}(\alpha')^{0.56}(1+2.1\beta^2)}, \quad (21)$$

where we remark again that we use the standard expression for $\Omega_m(a)$.

This new function is really a good approximation to the exact solution δ_{exact} , for different values of the coupling constant β , as one can see in Fig.1 where the curves of the growth factor $g \equiv \delta/a$ for two different β and the corresponding g_{fit} are plotted. In Fig.2 we present the level of accuracy of the fitting formula. As it can be seen we find fits to better than $\approx 1\%$ for different values of β . Moreover, we find that the best fit values of the parameters do not depend on the actual value of the present matter density $\Omega_{m,0}$. We experimented also with an inverse power-law potential and found that also in this case eq. (21) is a good fit (see curve for $\beta=0.1$ in Fig. 1). Without the η -correction the relative error $(\delta_{fit} - \delta_{exact})/\delta_{exact}$ becomes larger than 15% already for $\beta=0.2$.

V. COMPARING THE FIT TO THE OBSERVATIONS

In the previous section we have seen that the expression

$$s \equiv \Omega_m^{(s)}(\alpha)^\gamma(1+\eta), \quad (22)$$

where $\Omega_m^{(s)}(\alpha)$ is given by eq. (19) gives a good fit to the evolution of δ during both the decelerated and accelerated regimes for coupled dark energy models with constant $\beta < 1/2$ if $\gamma \approx 0.56$ and $\eta = 2.1\beta^2$. Here we take some preliminary steps towards comparing the fit (22) to the observations. An indication for a positive η could signal an attractive force additional to standard gravity as in a scalar-tensor model; on the other hand one can speculate that a negative η could be related to the slowed growth induced by a hot matter component.

We consider the following data: *a*) Lyman- α power spectra at an average redshift $z = 2.125$, $z = 2.72$ [23], $z = 3$ [24]; *b*) the normalization σ_8 inferred from Lyman- α at z ranging between 2 and 3.8 [25]; *c*) galaxy power spectra at low z from SDSS [26] and 2dF [27]. From the three Lyman- α and the SDSS spectra we estimate the ratios

$$r(k_i; z_1, z_2) = \frac{P(k_i, z_1)}{P(k_i, z_2)}, \quad (23)$$

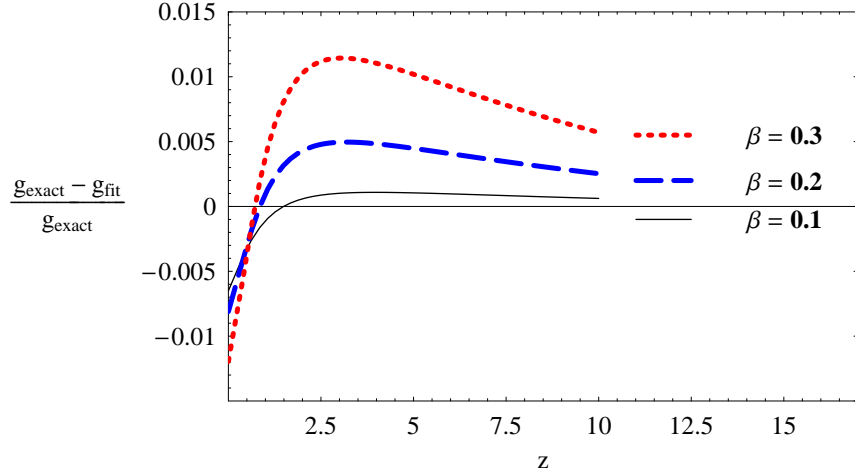


Figure 2: Level of accuracy of the best fit to the exact solution for the growth rate. For β ranging between 0 and 0.3 the fits are better than 1.2%. Without the correction the relative errors would be larger than 15% already for $\beta = 0.2$.

for the values of k_i for which there are tabulated value of the spectra (or for interpolated values and errors when the tabulated wavenumbers differ). For the σ_8 data we estimate the ratios between successive values of z ,

$$r(z_1, z_2) = \frac{\sigma_8^2(z_1)}{\sigma_8^2(z_2)} \quad (24)$$

(note that ref. [25] reports the values of σ_8 extrapolated at the present epoch).

For the Lyman spectrum at $z = 3$ and for 2dF ($z = 0.15$), the authors of [24, 27] give directly their estimation of the growth rate, $s_{obs} = 0.49 \pm 0.10$ for 2dF and $s_{obs} = 1.46 \pm 0.29$ for the Lyman- α data. Then we compare the observations to our fit by using the likelihood function

$$L = N \exp \sum_i \left(-\frac{(r_{i,obs} - r_{i,teor})^2}{2\sigma_i^2} \right) \exp \sum_j \left(-\frac{(s_{j,obs} - s_{j,teor})^2}{2\sigma_j^2} \right), \quad (25)$$

where the errors σ_i are obtained from the quoted errors on $P(k)$ and σ_8 by standard error propagation.

As we will see the data available at the present are not sufficient to set stringent limits to the growth function. Moreover, there are several sources of possible systematic effects that we cannot account for. For instance, the matter spectra derived from Lyman- α clouds are obtained through calibration (ie. bias correction) with N -body simulations; these simulations have been generated only for a limited set of cosmological models. It is difficult to quantify the impact of this limitation upon our results; the fact that we consider *ratios* of spectra from similar sources (eg Lyman- α clouds) might however alleviate the problem since one can expect that the calibration errors are only weakly dependent on redshift. For this reason we consider separately the ratios of the high- z Lyman- α spectra to the low- z SDSS galaxy spectra; our final results do not take these into account.

The current observational situation is summarized in Fig. (3) (and the associated Table I), in which we plot the data we used in this work, along with the Λ CDM growth rate and with our best fit (see below). This figure gives a clear idea of the potential for improvement in the observational estimation of the growth rate.

We assume that the function s depends on four parameters, $(\Omega_{m,0}, w_0, \gamma, \eta)$. We assume also a flat prior $\Omega_{m,0} \in (0.05, 0.4)$ and $w_0 \in (-1, -0.6)$ which generously accounts for the supernovae constraints (neglecting the phantom region). Our main result is contained in Fig. (5), which displays the likelihood contour plots at 68%, 95 and 99.7% in the plane (γ, η) , marginalizing over $\Omega_{m,0}, w_0$. Remarkably, the best fit values practically coincide with the Λ CDM prediction, $(\eta, \gamma) = (0, 0.6)$. However the likelihood extends considerably on both negative and positive η and even negative values of γ are not excluded beyond 3σ . In Figs. (6-7) we plot the marginalized 1D likelihoods for γ and η . The results are tabulated in Table II. The best fit values and 1σ errors are

$$\gamma = 0.60^{+0.41}_{-0.30}, \quad \eta = 0.00^{+0.28}_{-0.18}. \quad (26)$$

As we anticipated, the current data impose only very weak constraints on γ, η . For completeness, we also quote in Table II the best fit and errors on $\gamma_{standard}$, i.e. assuming a standard model in which $\eta = 0$. Even in this case the

z	s
ref. [23]	
2.125; 2.72	0.50; 0.98
ref. [25]	
2.2; 3	-1.147; 1.175
2.4; 3.2	-0.94; 1.198
2.6; 3.4	-0.686; 2.010
2.8; 3.6	-0.908; 1.778
3; 3.8	-1.207; 1.799
ref. [24]	
3	1.46 ± 0.49
ref. [27]	
0.15	0.49 ± 0.10

Table I: Summary of observational data. We report in the z and s columns either the corresponding ranges or the central value and errors. For the σ_8 data or ref. [25] we chose to report the errorboxes on s obtained using the ratios at the given redshifts.

	1σ	2σ	3σ
η	$0.00^{+0.28}_{-0.18}$	$+0.58_{-0.38}$	$+1.1_{-0.58}$
γ	$0.60^{+0.41}_{-0.30}$	$+0.97_{-0.49}$	$+1.6_{-0.74}$
$\gamma_{standard}$	$0.60^{+0.34}_{-0.26}$	$+0.77_{-0.40}$	$+1.4_{-0.50}$

Table II: Best fit and errors (marginalized over all other parameters).

likelihood distribution for γ remains very broad, although now negative values are rejected at more than 3σ . Including the ratio of Lyman- α to SDSS power spectra has a minor effect on γ and moves the best fit of η to -0.2 .

Assuming $\eta < 0.58$ at 2σ we can derive an upper limit to the coupling β introduced in Sect. 2,

$$\beta < 0.52 \quad (27)$$

(at 95% c.l.). This limit is very weak when compared to the CMB limits [18] but it is nevertheless interesting since it is independent and derived uniquely from the growth rate at small redshifts.

VI. CONCLUSIONS

The search for useful parametrizations of the dark dynamics is important since as it has been shown several times every parametrization introduces some arbitrariness in the way data are analysed [29]. In particular, with the advent of models of dark energy based on modification of Einstein's gravity, we have become aware of many possible trends, both at the background and at the perturbation level, that are not easily accounted for with earlier parametrizations. In this paper we introduced a generalized form of parametrization of the growth rate that allows for a rate $s \neq 1$, i.e. faster or slower than the standard matter-dominated growth. We show that this parametrization is suitable to model the fluctuation growth in coupled dark energy models and in scalar-tensor models.

We have analysed the current data in search of observational constraints on γ, η . Considering data from Lyman- α and galaxy power spectra at various redshifts we have obtained (rather weak) constraints on both parameters. The best fit turns out to be very close to the Λ CDM predictions. Many future experiments based on weak lensing or baryon oscillations will be able to estimate the growth rate and other fluctuation parameters with much higher precision [21, 22, 28]. We expect therefore that the constraints derived in this paper will soon be superseded by much more precise ones and that new estimates of the growth factor will help in clarifying the nature of dark energy.

Acknowledgments

We thank Enzo Branchini and Matteo Viel for useful discussions on the data analysis.

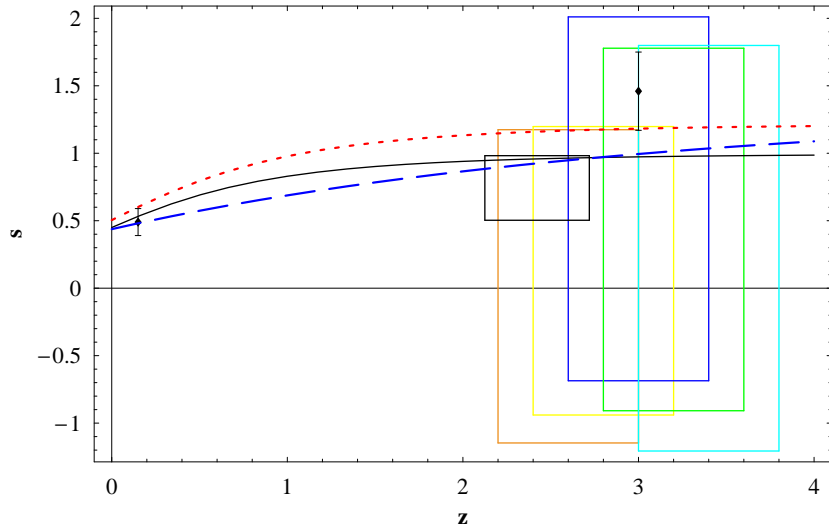


Figure 3: Summary of experimental data for the growth rate s , as detailed in Table I. The big coloured errorboxes represents the ratios $\sigma(z_1)/\sigma(z_2)$ for various z intervals of ref. [25] (three additional very large errorboxes have been excluded from the plot but not from the analysis); the smaller black box represents the average spectral ratio for the Lyman- α data of ref. [23]. The two points with errorbars are from ref. [27] and ref. [24]. The black solid line is the Λ CDM model, the red curve is the coupled dark energy model with $\Omega = 0.2$ and $\beta = 0.4$ (i.e. $\eta = 0.34$) and the dashed blue curve is the overall best fit $(\Omega_{m,0}, w_0, \gamma, \eta) = (0.05, -0.6, 0.4, 0.45)$.

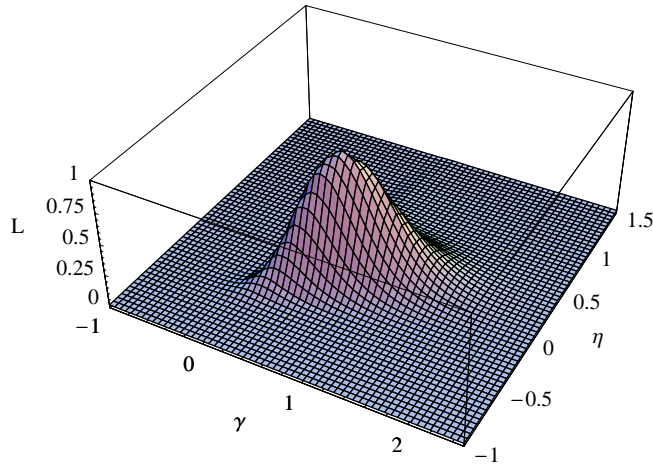


Figure 4: Tridimensional likelihood function marginalized on $\Omega_{m,0}$ and w_0 . The peak corresponds to $(\gamma, \eta) = (0.6, 0)$.

[1] A. G. Riess et al., *Astron. J.* **116**, 1009 (1998) astro-ph/9805201
[2] S. Perlmutter et al., *Astrophys. J.* **517**, 565 (1999) astro-ph/9812133
[3] P. Astier et al., *Astron. Astrophys.* **447** 31 (2006); T. M. Davis et al., astro-ph/0701510.
[4] D. N. Spergel et al. [WMAP collaboration], astro-ph/0603449 (2006).
[5] D. Eisenstein et al. [SDSS collaboration] *Astrophys. J.* **633**, 560 (2005) astro-ph/0501171
[6] S. Boughn and R. Crittenden, *Nature*, 427, 45 (2004)
[7] A. Réfrégier et al., astro-ph/0610062 (2006).
[8] A. Crotts et al., astro-ph/0507043 (2005).
[9] D. Parkinson et al. *MNRAS* 377, 185 (2007)
[10] O. Lahav et al. *MNRAS* **251**, 128 (1991)

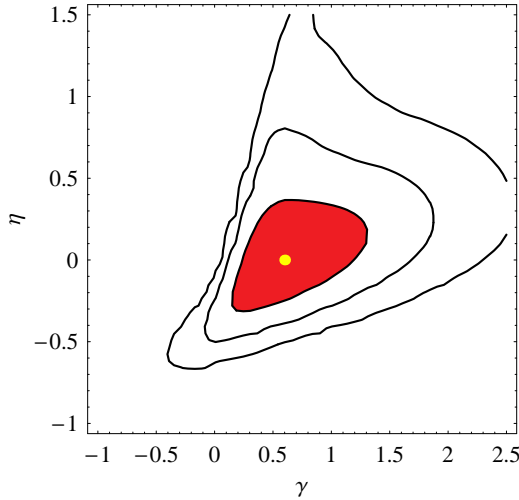


Figure 5: Contour plot of the likelihood marginalized over $\Omega_{m,0}$ and w_0 . The contours, from inside to outside, are at the 68% (red zone), 95%, 99.7% confidence level. The dot marks the peak $(\gamma, \eta) = (0.6, 0)$.

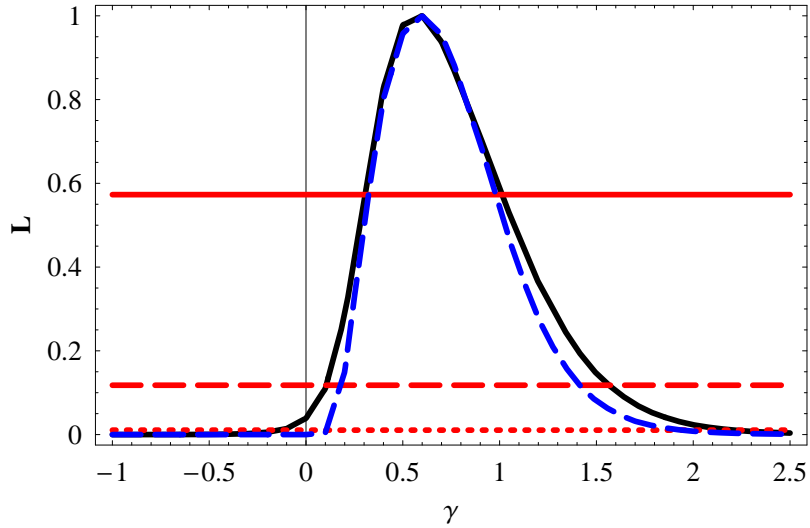


Figure 6: Marginalized likelihood for γ (solid line) and for γ_{standard} , i.e. fixing $\eta = 0$ (dashed line). The three horizontal lines represent the 68, 95, 99.7% c.l. from top to bottom.

- [11] L. Wang & P. J. Steinhardt, *Astrophys. J.* **508**, 483 (1998).
- [12] L. Amendola & C. Quercellini, *Phys. Rev. Lett.* **92**, 181102 (2004)
- [13] E. V. Linder, [astro-ph/0507263](#)
- [14] S. Dodelson, M. Liguori, *Phys. Rev. Lett.*, (2006) 97, 231301
- [15] T. Damour, G. W. Gibbons, C. Gundlach, *Phys. Rev. Lett.*, 64, 123 (1990); T. Damour, C. Gundlach, *Phys. Rev. D* 43, 3873 (1991)
- [16] C. Wetterich, *A&A*, 301, 321 (1995)
- [17] L. Amendola, *Phys. Rev. D* **62**, 043511 (2000)
- [18] L. Amendola, C. Quercellini, *Phys. Rev. D* **68**, 023514 (2003)
- [19] L. Amendola, R. Gannouji, D. Polarski, S. Tsujikawa, *Phys. Rev. D* 75:083504, 2007. [[gr-qc/0612180](#)]
- [20] L. Amendola *Phys. Rev. D* 69:103524, 2004. [[astro-ph/0311175](#)]
- [21] L. Amendola, M. Kunz, D. Sapone (2007) [arXiv:0704.2421](#);
- [22] R. Caldwell, A. Cooray and A. Melchiorri (2007) [astro-ph/0703375](#)
- [23] M. Viel, M. G. Haehnelt, V. Springel, *MNRAS* **358**, 684-694 (2004)
- [24] Mc Donald et al., [astro-ph/0407377](#)
- [25] M. Viel & M. G. Haehnelt, 2006, *MNRAS*, 365, 231

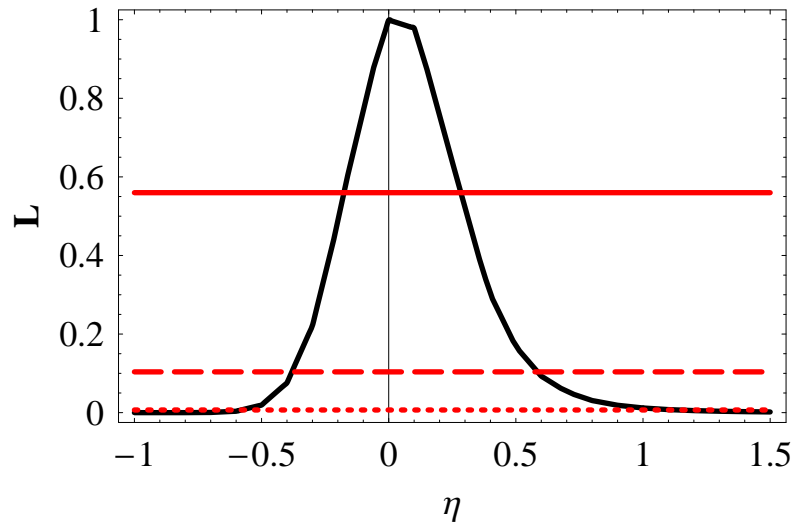


Figure 7: Marginalized likelihood for η . The three horizontal lines represent the 68,95,99.7% c.l. from top to bottom.

- [26] M. Tegmark et al. Ap.J. 606, 702 (2004)
- [27] M. Colless et al., MNRAS **328** 1039 (2001)
- [28] D. Huterer and E.V. Linder, Phys. Rev. D **75**, 023519 (2007).
- [29] B. Bassett, P. Corasaniti & M. Kunz, ApJ 617, L1 (2004) astro-ph/0407364